# Thermal conductivity measurement under hydrostatic pressure using the 3$\omega$ method

Feng Chen,[a] Jason Shulman, Yuyi Xue, and C. W. Chu[b]
*Texas Center for Superconductivity and Advanced Materials, University of Houston, Houston, Texas 77204-5002*

George S. Nolas
*Department of Physics, University of South Florida, Tampa, Florida 33620*

(Received 16 June 2004; accepted 24 August 2004; published 29 October 2004)

We have designed and modeled new techniques, based on the 3$\omega$ method, to measure thermal conductivity of liquids ($\kappa_l$) and solids ($\kappa_s$) under hydrostatic pressure ($P$). The system involves a solid sample immersed in a liquid pressure medium, both of which have unknown thermal properties. The temperature ($T$) and $P$ dependance of $\kappa_l$ are first determined through the use of a modified 3$\omega$ technique. This method uses a conducting wire (Pt, in this work), which is immersed in the pressure medium, as the heater/sensor. In addition to $\kappa_l$, this allows for the accurate determination of the specific heat per volume of the liquid and Pt, $(\rho C)_l$ and $(\rho C)_{\mathrm{Pt}}$, respectively. The information of $\kappa_l$ and $(\rho C)_l$ can then be used to make corrections to measurements of $\kappa_s$, in which the sample is immersed in the pressure medium, and a metal strip acts as the heater/sensor. We present the $T$ and $P$ dependence of $\kappa_l$ and $(\rho C)_l$ for the widely used pressure medium 3M Fluorinert FC77 up to 0.8 GPa. The measurement of $\kappa_s$ for a thermoelectric clathrate material, $Sr_8Ga_{16}Ge_{30}$, in FC77 is analyzed in detail, and the refined data achieves an accuracy of 1%. The setup can be modified to measure $\kappa$ and $\rho C$ up to 3.5 GPa. © *2004 American Institute of Physics.* [DOI: 10.1063/1.1805771]

## I. INTRODUCTION

Measuring thermal transport properties of solid samples under hydrostatic pressure presents a technical challenge due to the large heat loss associated with the pressure medium. The heat flux though the pressure medium, e.g., 3M Flourinert FC77, at the room temperature is comparable to that through a Pyrex glass sample of $1\times1\times10\ \mathrm{mm}^3$ in the steady-state method. The complicated geometry, the possibility of convection, and the deformation associated with pressure make the related corrections difficult if not impossible. The transient method has been proposed to overcome the problems.[1] In this measurement, a heater and a sensor are positioned either between two identical solid samples (so-called pseudoinfinite specimen) or on the surface of the sample immersed in liquid medium. The temperature relaxation, after a heating pulse, is measured by the sensor. The relaxation profile, which can be described as a 2D thermal diffusion through either a homogeneous medium or two half-space media, can be mathematically fit with the thermal conductivity $\kappa$ and the volume thermal capacitance $\rho C$ as free parameters, where $\rho$ and $C$ are the density and the mass thermal capacitance, respectively. The heat loss is reduced, and an accurate correction is possible due to the simple geometry of the system. The same transient method has been used to measure the $\kappa_l$ of liquid.[2] Fast and accurate temperature sampling, however, becomes the key in such relaxation profile measurements. The integral time constant (i.e., the high frequency cutoff) and the associated sensitivity of the voltmeter in turn set the limits for the spacial resolution and the pulse power, respectively. Although reasonable accuracy was reached, improvement is highly desired. The 3$\omega$ method[3,4] offers a more convenient way to realize the thermal transport inside a pressure medium. A similar arrangement of heater-on-surface is typically used in this method. The sample is heated by sending an ac current of angular frequency $\omega$ through a metal strip. The temperature is deduced from the third harmonic voltage across this heater. The conflict that exists in the transient method between a fast response and a high sensitivity is largely overcome by the ac lock-in technique. Extremely small sample size as well as space-resolvable measurement in the multilayer configuration are possible. The faster time window adopted also largely suppresses the interference from convection, whose effect decreases with frequency.

The correction for the heat lost to the liquid is still needed, however, without adopting the inconvenient pseudoinfinite geometry. Previously, the "boundary mismatch" model has been proposed to take this correction into account.[5] The total thermal flux is regarded as the summation of the flows into the semi-infinite space of the sample and that of the liquid, with a ratio which requires the average temperatures at two surfaces of the heater to be equal. Essentially, the model ignores the thermal flux across sample-medium boundary, which is reasonable if the two

[a]Author to whom correspondence should be addressed; electronic mail: fchen@uh.edu
[b]Also at: Lawrence Berkeley National Laboratory, Hong Kong University of Science and Technology.

 

have similar values of $\kappa/\rho C$. A further simplification, as will be discussed below, was adopted, and a simple equation, $\kappa_{s+l}=\kappa_l+\kappa_s$, follows. Here, $\kappa_{s+l}$, $\kappa_l$, and $\kappa_s$ are the conductivities of the apparent sample-medium combination, the liquid medium, and the solid sample, respectively. However, the justification for this simple correlation is only approximate, and our improved experimental resolution enables us to introduce a higher order correction, which eliminates the modeling uncertainty to around 1%.

To improve upon the procedure of measuring $\kappa_s$ under pressure, a modified version of the $3\omega$ method has been developed to accurately determine the thermal properties of the dielectric liquid under pressure. Once the thermal properties of the pressure medium have been calibrated under pressure, these values are incorporated into a standard $3\omega$ measurement, which utilizes a *corrected* boundary mismatch approximation. In addition, the $\kappa_s$ at the ambient pressure was independently measured and the boundary mismatch model was experimentally verified. Our results suggest that $\kappa_s$ under pressure can be deduced with a possible deviation less than a few percent.

## II. EXPERIMENTAL SETUP AND INSTRUMENTATION

The hydrostatic pressure is generated inside a Teflon cell, housed in a Be–Cu high pressure clamp.[6] The electrical leads are Pt wires attached to the heater/thermometer by silver epoxy (EPO-TEC H20E). These leads are soldered to wires with enamel insulation that are fed through a #72 hole and sealed by epoxy. The 3M Fluorinert FC77 is used as the pressure medium in order to achieve highly *hydrostatic* pressure. The pressure was calculated by the force over area at room temperature. Our previous experiments used superconducting Pb as a magnometer to measure pressure near liquid helium temperature and demonstrated that the pressure obtained using this method is within 10% throughout the temperature range of 4 K to 300 K.[7] This setup can be modified to obtain hydrostatic pressure up to 3.5 GPa.[8]

The $3\omega$ setup has been documented in detail by Cahill.[4] In brief, a narrow, thin metal strip is deposited on the surface of the sample. This strip is used as both heater and temperature sensor. An ac signal of angular frequency $\omega$ flows through the strip and generates heat at the angular frequency $2\omega$. This heat further induces a temperature fluctuation, which is limited by the thermal diffusion of the sample. This temperature fluctuation can be measured through the heater's resistance ($R$), if its temperature ($T$) dependence is known. In the most simple case of a linear $R-T$ correlation, the third harmonic component of the voltage across the heater will represent the temperature fluctuation. Measuring the frequency ($f$) dependence of this $3\omega$ voltage, therefore, allows both $\kappa$ and $\rho C$ to be determined since the thermal diffusion of solids, i.e., the "cooling power" of the sample, varies with $\kappa$, $\rho C$, and $\omega$ in a well defined way.

We use two different $3\omega$ setups for measuring $\kappa_s$ and $\kappa_l$. The measurement of $\kappa_s$ is similar of that of Cahill's, except that in our case the sample is immersed in the pressure medium FC77. To measure $\kappa_l$, a Pt wire of radius $a=5.0$ $\mu$m and length $l\approx 7$ mm is immersed in the pressure medium. This wire now acts as the heater/thermometer. The heat transport equation can be solved exactly in a 2D cylindrical geometry. The $3\omega$ signal is then fit to this solution to deduce $\kappa_l$, $(\rho C)_l$ and $(\rho C)_{\mathrm{Pt}}$. The measurements have been carried out for FC77 at several pressures.

The measurement of the $3\omega$ signal is achieved using a Stanford Research SR830 digital lockin amplifier, which can measure multiple harmonics of the reference signal. It should be pointed out that the $3\omega$ signal is typically $10^4$ times weaker than the fundamental $1\omega$ signal, therefore an analog balance circuit is necessary. A constant amplitude ac current source is also desired. A programmable balance bridge with very low $3\omega$ distortion is preferred since the balance varies significantly with the sample temperature. A homemade circuit box was built and is shown in Fig. 1. $V_{1f}$ is the ac voltage output of the SR830 at the frequency $\omega=2\pi f$. The unit U1 is an instrumentation amplifier that converts the ac voltage source to an ac current source. The ac current with constant amplitude is fed to the serially connected $R_{3f}$ (the heater/sensor that generates $3\omega$ signal) and $R_{\mathrm{pot}}$ (a 100 $\Omega$ adjustable potentiometer). The voltage across $R_{3f}$ is supplied to a unity-gain differential amplifier U2. The signal is then fed into one of the differential inputs of the SR830 (A). The voltage output from $R_{\mathrm{pot}}$, which should be proportional to the $1\omega$ component across $R_{3f}$, is supplied to the unit U3, a 12-bit multiplying DAC that is controlled by an IBM PC parallel port. This unit, together with the buffer unit U4, enables the automation of the balancing of the $1\omega$ signal with varying temperature. The signal is then fed into another differential inputs of SR830 (B). Using this setup, the $1\omega$ signal from A can be measured to calibrate the curve $R(T)$, together with the average sample temperature; the $1\omega$ signal from the differential signal, A–B, can be minimized. The $3\omega$ component from the signal A–B is finally measured. This process is entirely computer controlled, and there is no need for physical rewiring.

## III. CONFIGURATIONS AND MODELING

We designed two different configurations for $3\omega$ thermal conductivity measurements. To measure $\kappa_s$ for a solid sample, a finite-width strip heater/sensor, which is at the interface between the solid sample and liquid medium is used. In order to calibrate $\kappa_l$ under high pressure, a different configuration with a metal wire heater/sensor surrounded by the liquid pressure medium is adopted. In Sec. III A 1 we briefly discuss the most general $3\omega$ configuration, which is a finite-width strip on a semi-infinite medium. Then, we generalize to the case in which the strip is on the interface between two semi-infinite media in Sec. III A 2. In Sec. III B we give the solution for the new $3\omega$ configuration in which the heater/sensor is a wire immersed in the pressure medium.

All the ac values have a time-dependent factor of $e^{im\omega t}$ with $m=1$, 2, and 3 for excitation voltage ($V$), excitation power ($P$) or temperature rise ($\delta T$), and the $3\omega$ voltage ($V_{3\omega}$), respectively. For convenience, this factor will be ignored in what follows. Each value is typically complex, with the real part being the in-phase component and the imaginary part being out-phase component. The dc component will be

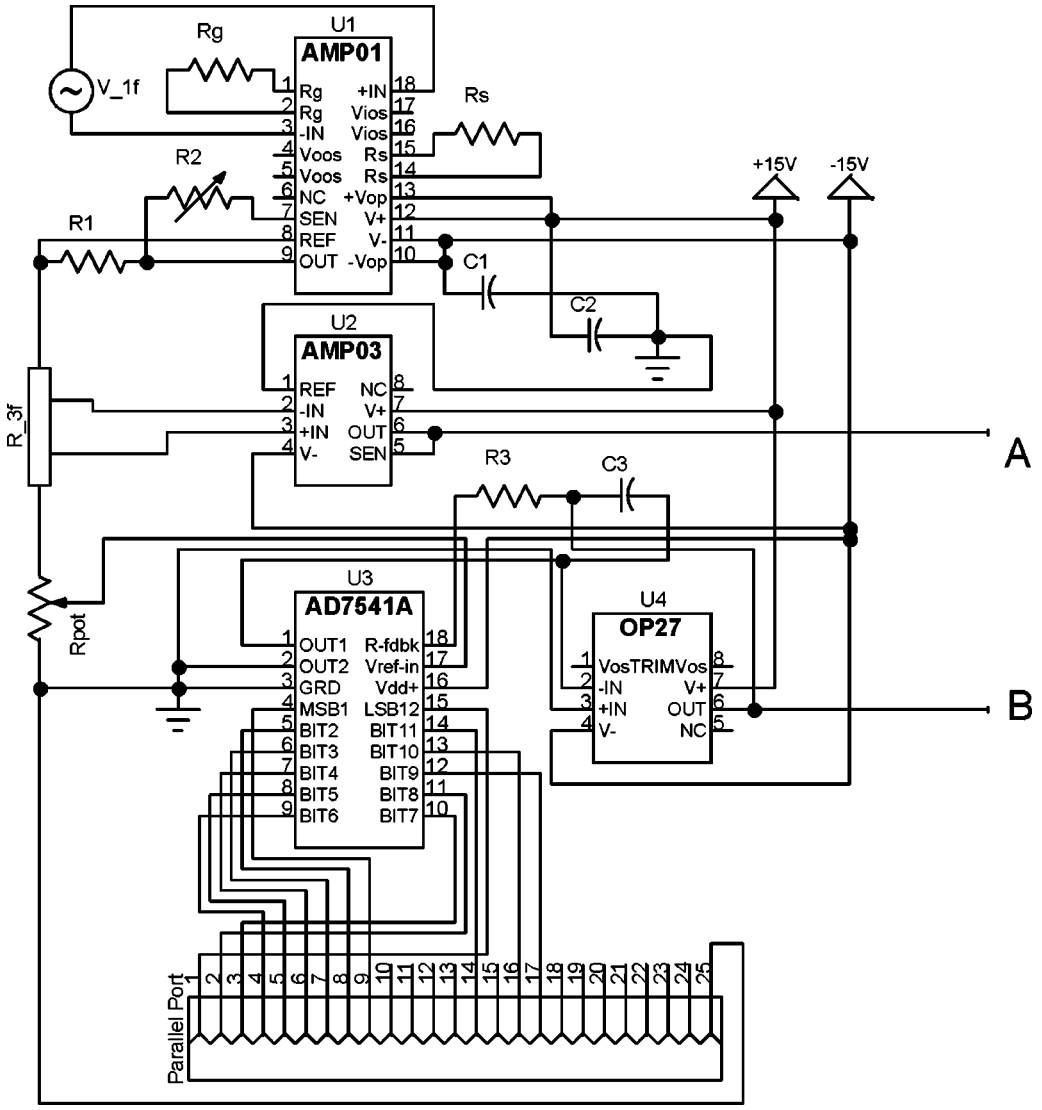


FIG. 1. The circuit diagram for a homemade electronic box for a $3\omega$ measurement. The units U1–U4 are AMP01, AMP03, AD7541A, and OP27 from analog devices, respectively. $R_g=10$ kΩ, $R_s=500-2000$ Ω, $R_1=100$ Ω, $R_2=200$ Ω, $R_{\text{pot}}=100$ Ω, $R_3=33$ Ω, $C_1=C_2=10$ pF, and $C_3=33$ pF. The outputs A and B are connected to the A and B connectors of an SR830 lockin. Note that the unit U1 has a high frequency cutoff of 2 kHz in practice and should be replaced by an amplifier with a wider bandwidth if higher frequency is desired.

ignored since it does not contribute to the final $V_{3\omega}$, and therefore, the thermal conductivity determination.

### A. The $3\omega$ method with a finite-width strip heater

#### *1. A finite-width strip heater on the surface of a semi-infinite medium*

Consider an infinitely thin and infinitely long heater on the surface of a semi-infinite medium of thermal conductivity $\kappa$. The ac power per unit length used to heat this line is $P_L$. The steady-state solution to the heat equation of the system is a thermal wave of the form[9]

$$\delta T(r) = \frac{P_L}{\pi\kappa} K_0(qr), \tag{1}$$

where $K_0$ is the zeroth order modified Bessel function, and $q=\sqrt{(2\omega\rho C/\kappa)i}$.

In practice, the heater will have a finite width, $2b$, so the appropriate superposition of solutions, of the form of Eq. (1), is needed. The steady-state solution for the average temperature on the heator/sensor then becomes[4]

$$\delta T = \frac{P_L}{\pi\kappa}\int_0^\infty \frac{\sin^2(kb)}{(kb)^2(k^2+q^2)^{1/2}}dk = \frac{P_L}{\pi\kappa}\mathcal{F}(qb), \tag{2}$$

where

$$\mathcal{F}(\psi) = \int_0^\infty \frac{\sin^2\phi}{\phi^2(\phi^2+\psi^2)^{1/2}}d\phi. \tag{3}$$

When $b\to\infty$, the problem becomes 1D and the solution is $(P_A/\sqrt{2\omega\rho C\kappa})e^{-i(\pi/4)}$, where $P_A=P_L/2b$ is the power per unit area.

In most cases, there will be an interfacial thermal resistance $\mathcal{R}$ between the strip and the sample. In the case of a

thin insulating layer with an electrically conducting sample, the effect of the layer can also be approximated by an effective $\mathcal{R}$. Equation (2) then becomes

$$\delta T = \frac{P_L}{\pi\kappa}\mathcal{F}(qb) + \frac{P_L\mathcal{R}}{2b}. \tag{4}$$

#### 2. A finite-width strip heater on the boundary of two semi-infinite media

Now let us consider the case that the strip heater is on the boundary of two semi-infinite media $s$ and $l$. We denote the corresponding physical properties of these two media by subscript with $s$ and $l$, respectively, if no further notes are given.

In the 1D case, the solution can be simply obtained by defining the power dissipated to medium $s$ and medium $l$ to be $P^{(s)}$ and $P^{(l)}$, respectively, so that $P=P^{(s)}+P^{(l)}$. The ratio of $P^{(s)}$ and $P^{(l)}$ can be determined by equalizing the average boundary temperatures: $\delta T^{(s)}=\delta T^{(l)}$. The final solution is[5]

$$\delta T = \frac{P_A}{\sqrt{2\omega\rho_s C_s\kappa_s}+\sqrt{2\omega\rho_l C_l\kappa_l}}e^{-i(\pi/4)}. \tag{5}$$

For the general 2D case, a boundary mismatch model has been previously proposed.[5] This approximation models the problem as two separate semi-infinite media without heat flow across the boundary. Only the average temperatures on the strip are made equal, while the temperature mismatch at the boundary is tolerated. It has been further assumed that $\kappa_{s+l}=\kappa_s+\kappa_l$.[5] $\kappa_{s+l}$ is the apparent thermal conductivity of the two media combination, which is treated by fitting the data as if there is only one semi-infinite medium. In this article, $\kappa_{s+l}$ is defined as the apparent thermal conductivity by fitting the real part of Eq. (2) or 4 with parameters $\kappa_{s+l}$, $q_{s+l}$, and $\mathcal{R}$ in the case of Eq. (4).

However, an improved solution can be deduced even under the boundary mismatch approximation. The same energy conservation $P=P^{(s)}+P^{(l)}$ combined with Eq. (2) actually leads to

$$\frac{1}{\delta T_{s+l}} = \frac{\pi\kappa_s}{P_L\mathcal{F}(q_s b)} + \frac{\pi\kappa_l}{P_L\mathcal{F}(q_l b)}. \tag{6}$$

This equation can be further converted to

$$\frac{\pi\kappa_{s+l}}{P_L\mathcal{F}(q_{s+l}b)} = \frac{\pi\kappa_s}{P_L\mathcal{F}(q_s b)} + \frac{\pi\kappa_l}{P_L\mathcal{F}(q_l b)}, \tag{7}$$

or,

$$\frac{1}{\delta T_{s+l}} = \frac{1}{\delta T_s} + \frac{1}{\delta T_l}. \tag{8}$$

Note the difference between the notations with superscript or subscript for $P$ or $\delta T$, e.g., $\delta T^{(s)}$ and $\delta T_s$. For the superscript case, the values are for the same measurement in the two media configuration, thus $\delta T^{(s)}=\delta T^{(l)}=\delta T_{s+l}$; while for the subscript case, the values $\delta T_{s+l}$, $\delta T_s$ and $\delta T_l$ are from three different measurements with two media, single medium $s$ and homogeneous medium $l$ respectively, with power $P_L$. In the case that the same heator/sensor is used, Eq. (8) can be further expressed in terms of the $3\omega$ voltage:

$$\frac{1}{V_{s+l}} = \frac{1}{V_s} + \frac{1}{V_l}. \tag{9}$$

Without loss of generality, we can assume $\kappa_s \geqslant \kappa_l$. It is natural to approximate Eq. (7) to

$$\kappa_{s+l} = \kappa_s + \alpha\kappa_l, \tag{10}$$

with the assumption $\mathcal{F}(q_{s+l}b)\approx\mathcal{F}(q_s b)$, and $\alpha = \mathcal{F}(q_{s+l}b)/\mathcal{F}(q_l b)$ under the boundary mismatch approximation. In fact, Eq. (10) is a handy generic formula since $\alpha$ can be artificially adjusted to correct the boundary mismatch approximation, the approximation that $\mathcal{F}(q_{s+l}b)\approx\mathcal{F}(q_s b)$, and the small variation in $\alpha$ with $f$.

A matrix formalism provides an exact solution for the case of a strip-heater between two media, even with a nonzero interfacial thermal resistance, $\mathcal{R}$, between the strip and the solid sample.[10] The solution is

$$\delta T = \frac{P_L}{\pi}\int_0^\infty \frac{\sin^2(kb)}{kb}\frac{1+\gamma_s\mathcal{R}}{\gamma_l+\gamma_s+\gamma_l\gamma_s\mathcal{R}}dk, \tag{11}$$

where $\gamma_i=\kappa_i\sqrt{k^2+q_i^2}$. Compared to this exact solution, Eq. (10) is a simple and intuitive way to estimate both the value and the error of $\kappa$.

### B. $3\omega$ wire method to measure $\kappa_l$

#### 1. Solution of the 2D diffusion equation

Consider a Pt wire of length $l$ and diameter $a$ which is immersed in an electrically insulating liquid. An ac heating voltage of $V$ is supplied. In the case of $l \gg a$, the system can be treated as 2D. We assume that the heat transferred by liquid flow is negligible and that the heating is uniform over the Pt wire, such that the power per unit volume $(P_V)$ is $(1/\pi a^2 l)(V^2/R)$, where $R$ is the resistance of the Pt wire. Due to symmetry, in the cylindrical 2D subspace $(r,\theta)$, the steady-state temperature is $T(r)$. If we use index 1 to denote $r \leqslant a$ and 2 for $r > a$, we have

$$\frac{d^2T_1}{dr^2} + \frac{1}{r}\frac{dT_1}{dr} - q_1^2 T_1 = -\frac{P_V}{\kappa_1}, \tag{12}$$

$$\frac{d^2T_2}{dr^2} + \frac{1}{r}\frac{dT_2}{dr} - q_2^2 T_2 = 0, \tag{13}$$

where $q_1=\sqrt{(2\omega\rho_1 C_1/\kappa_1)i}$ and $q_2=\sqrt{(2\omega\rho_2 C_2/\kappa_2)i}$.

The exact solution exists analytically:

$$T_1 = \eta I_0(q_1 r) + \frac{P_V}{\kappa_1 q_1^2}, \tag{14}$$

$$T_2 = \xi K_0(q_2 r), \tag{15}$$

where $I_0$ and $K_0$ are the zeroth order modified Bessel functions.

The parameters $\eta$ and $\xi$ can be determined by requiring that the temperature and the heat flux are continuous at the boundary $r=a$:

$$\eta I_0(q_1 a) + \frac{P_V}{\kappa_1 q_1^2} = \xi K_0(q_2 a), \tag{16}$$

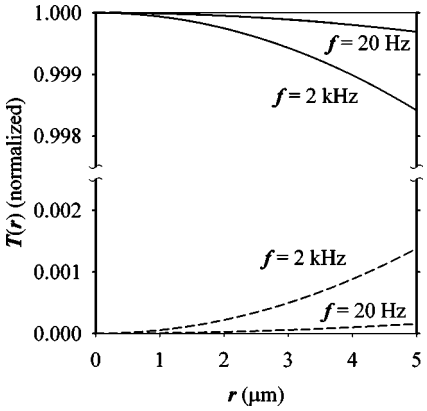


FIG. 2. Normalized temperature variation along the radius of the Pt wire at frequencies $f=20$ Hz and 2000 Hz. The solid lines are the real parts and the dashed lines are the imaginary parts. The values used here are $\kappa_1=71.6\ \mathrm{W\,m^{-1}\,K^{-1}}$, $\rho_1=21.4\times10^3\ \mathrm{kg/m^3}$, $C_1=130\ \mathrm{J/kg\,K}$, $\kappa_2=0.063\ \mathrm{W\,m^{-1}\,K^{-1}}$, $\rho_2=1.1\times10^3$, $C_2=1.78\times10^3\ \mathrm{J/kg\,K}$.

$$-\eta\kappa_1 q_1 I_1(q_1 a)=\xi\kappa_2 q_2 K_1(q_2 a), \tag{17}$$

where $I_1$ and $K_1$ are the first order modified Bessel functions.

#### 2. A simplification of the exact solution

Recall that we assume that the heating power is distributed uniformly throughout the Pt wire, and the temperature variation across the Pt wire is negligible. This assumption is natural since $\kappa_1$ of the Pt wire is rather high and $r$ is small, thus $|q_1 a|\ll 1$ and $I_0(q_1 r)$ is almost constant when $r\leqslant a$. To demonstrate this, we plot the real part and imaginary part of $T_1(r)/|T_1(0)|$ at the frequencies 20 Hz and 2000 Hz for $0\leqslant r\leqslant a$, where $a=5.0$ $\mu$m (Fig. 2). The result shows the deviation is less than 0.2% even for our highest frequency. Therefore, the assumption is verified. Furthermore, we can treat $T_1(a)$ or $T_2(a)$ as the average temperature of the Pt wire.

Since $|q_1 a|\ll 1$ is well satisfied, we can approximate the boundary conditions in Eqs. (16) and (17) to

$$\eta+\frac{P_V}{\kappa_1 q_1^2}=\xi K_0(q_2 a), \tag{18}$$

$$-\tfrac{1}{2}\eta\kappa_1 q_1^2 a=\xi\kappa_2 q_2 K_1(q_2 a). \tag{19}$$

This gives the same result derived by Birge[11]

$$T_2(a)=\frac{P_V a^2}{2\kappa_2 q_2 a\dfrac{K_1(q_2 a)}{K_0(q_2 a)}-\kappa_1(q_1 a)^2} \tag{20}$$

or, in a format that is easy to fit vs frequency,

$$T_2(a)=\frac{P_V a^2}{2\kappa_2\sqrt{\dfrac{f}{f_2}}(1+i)\dfrac{K_1\left(\sqrt{\dfrac{f}{f_2}}(1+i)\right)}{K_0\left(\sqrt{\dfrac{f}{f_2}}(1+i)\right)}+i4\pi a^2\rho_1 C_1 f}, \tag{21}$$

where $f_2=(1/2\pi a^2)(\kappa_2/\rho_2 C_2)$.

Compared to the exact solution [Eq. (14)] with four unknown parameters, the approximate solution [Eq. (20)] has only three unknown parameters. As we will discuss with the data [Eq. (20)] is not only more suitable for data fitting, but also more physically intuitive.

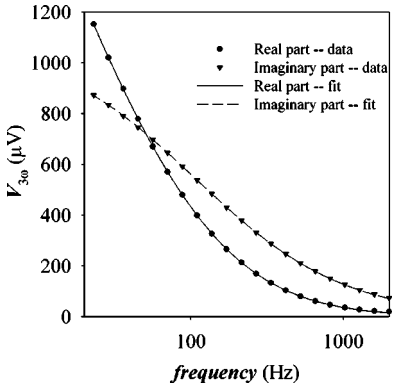


FIG. 3. Real and imaginary parts of the $3\omega$ voltage vs the logarithm of frequency. The solid circles represent the real part of the $3\omega$ voltage, the solid triangles represent the negative imaginary part of the $3\omega$ voltage. The solid and dashed lines are the fit using Eq. (21).

## IV. DATA AND NUMERICAL FITTING

### A. Thermal conductivity of the liquid FC77

In order to adapt the $3\omega$ method to a wire in a small pressure cell containing a pressure medium, we chose Pt wire with a radius of 5.0 $\mu$m and $\sim$7 mm long. The wire, which is connected to electrical leads by silver epoxy, is manageable but still has a reasonable 10 $\Omega$ 4-wire resistance at room temperature. As estimated from Sec. III B 2, the temperature along the radius of the Pt wire can be treated as constant (Fig. 2), but the heat capacity of the Pt wire can no longer be ignored.

The $3\omega$ voltage vs frequency for the Pt wire immersed in FC77 at room temperature is plotted in Fig. 3. The symbols are experimental data and the curves are the fittings using Eq. (21). We can see that the model fits the data well without inclusion of the interfacial thermal resistance between the wire and the liquid. The $\kappa_2$ obtained for FC77 is $0.063\ \mathrm{W\,m^{-1}\,K^{-1}}$, in good agreement with the data from the manufacturer. The value of $\rho_2 C_2$ obtained for FC77 is $2.1\ \mathrm{J/cm^3}$, and $\rho_1 C_1$ for Pt is $2.9\ \mathrm{J/cm^3}$, both in good agreement with known values of the respective materials.

It is obvious that the first term in the denominator of Eq. (20) is determined by the properties of the material surrounding the Pt wire, and the second term is contributed by Pt wire. In fact, this first term is the solution given by Carslaw and Jaeger,[12] provided that the heat flux at the boundary equals $P_V a/2$, i.e., when the heat capacitance of the Pt wire is ignored. A close look at the second term in the denominator of Eq. (21) shows that it is only a function of $\rho_1 C_1$, while the value of $\kappa_1$ is insignificant. In fact, the approximation adopted in Sec. III B 2 is essentially the assumption that $\kappa_1\gg 2\pi a^2 f\rho_1 C_1$. Equation (21) also shows that when one wants to obtain more accurate information on the value $\kappa_2$, the frequency range should cover frequencies low enough compared to $f_2$, in our case 30–120 Hz. Frequencies higher than $f_2$ are required to determine reliable information on $\kappa_2/\rho_2 C_2$ when the magnitude of the interface thermal resistance is

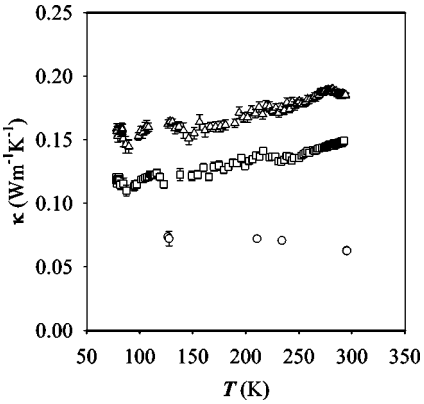


FIG. 4. $\kappa_l$ vs $T$ at different $P$ for the pressure medium FC77. (Circles: $P=0.0$ GPa, squares: $P=0.4$ GPa, triangles: $P=0.8$ GPa.)

large and unknown. The frequency $f^*$, at which the real and imaginary parts of $T_2(a)$ are equal, is rather difficult to determine. However, simulations indicate that it will not differ greatly from $f_2$. This method can, in principle, be adopted to measure heat capacity of nanowires, although, one must be aware that $f^* \sim f_2 \propto a^{-2}$ and could be a challenge for very small $a$.

Figure 4 shows the $\kappa_l$ vs $T$ for FC77 at various pressures. We can see that $\kappa_l$ increases with pressure from 77 K to 300 K. The large data scattering at low temperature region is due to the drifting of the temperature during the measurement. Greater control of the temperature will improve the data fluctuation to within 1%, as demonstrated for data near room temperature, where the temperature drifting is slower. For room temperature values, $\kappa_l$ increases from 0.06 W m$^{-1}$ K$^{-1}$ to 0.18 W m$^{-1}$ K$^{-1}$ when pressure is increased from 0.0 GPa to 0.8 GPa. The sign of $\partial\kappa(T,P)/\partial T$ is negative for $P=0.0$ GPa, which is consistent with the manufacturer's data. However, the overall $\partial\kappa(T,P)/\partial T$ becomes positive for $P=0.4$ and 0.8 GPa. The change of sign for $\partial\kappa(T,P)/\partial T$ near room temperature for $P=0.8$ GPa is coincident with the glass transition of FC77 under high pressure.[13] Similar data were discussed in detail by Birge.[11] In fact, the glass transition effect is more prominent in the $\rho C$ data. Figure 5 shows the $(\rho C)_l$ vs $T$ at various pressures. The only notable change under pressure are the peaks around

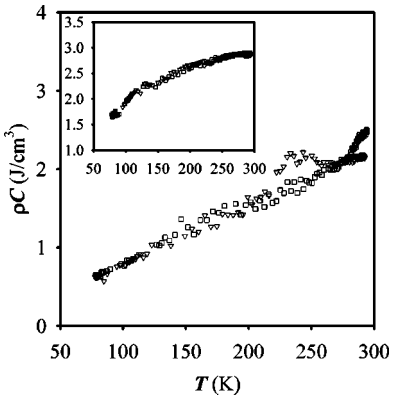


FIG. 5. $\rho C$ vs $T$ at different $P$ for the pressure medium FC77. Inset: $\rho C$ vs $T$ at different $P$ for the Pt wire extracted from the same data set. (Squares: $P=0.4$ GPa, triangles: $P=0.8$ GPa.)

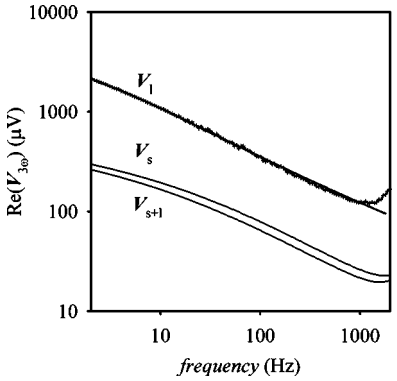


FIG. 6. A demonstration of using boundary mismatch approximation to solve $\kappa_l$ using a relative method. $V_l$ was obtained from $V_{s+l}$ and $V_s$. The solid line is the fit using Eq. (4) and gives a value of $\kappa_l = 0.090 \pm 0.003$ W m$^{-1}$ K$^{-1}$.

240 K at $P=0.4$ GPa and around room temperature at $P=0.8$ GPa. Evidence that the anomalies are due to the glass transition of the FC77 can be seen in the inset of Fig. 5. Here, $(\rho C)_{\mathrm{Pt}}$, which was obtained together with $(\rho C)_l$, is plotted versus temperature at the previously mentioned pressures. No anomalies are detected around the corresponding temperature regions, thus demonstrating that the peaks in the $(\rho C)_l(T)$ curves are not experimental artifacts.

This wire-heater method can also be applied to measure the thermal conductivity of solids if the heater can be embedded in the sample with good thermal contact. It can also be generalized for an electrically conducting liquid if the insulation issue can be handled, and if the extra thermal resistance due to insulating layer is considered/modeled. The wire-heater method can also be used to measure $\rho C$ of nanowires if high enough frequencies can be achieved.

### B. Thermal conductivity of solid samples

A clathrate ($Sr_8Ga_{16}Ge_{30}$) sample was measured both with and without FC77 medium at ambient pressure. The heater/thermometer is $\sim 90$ $\mu$m wide and insulated from the sample by a $SiO_2$ layer that is $\sim 1$ $\mu$m thick. As an example, the $3\omega$ voltages $V_{s+l}$, $V_s$ and $V_l = 1/((1/V_s)-(1/V_{s+l}))$ at the ambient pressure are shown in Fig. 6. For simplicity, only the real parts of the $3\omega$ voltages are plotted. Over the entire frequency range, the experimental resolution is much better than the difference $(1/V_s(\omega))-(1/V_{s+l}(\omega))$, which enables us to quantitatively evaluate the deviation for both the boundary mismatch model [Eqs. (6)–(9)] and the approximation $\kappa_{s+l} = \kappa_l + \kappa_s$. Fitting the values $V_s$, $V_{s+l}$, and $V_l$ by Eq. (4) gives values of $\kappa_s = 1.25$ W m$^{-1}$ K$^{-1}$, $\kappa_{s+l} = 1.35$ W m$^{-1}$ K$^{-1}$ and $\kappa_l = 0.090$ W m$^{-1}$ K$^{-1}$. Thus, $\kappa_l$ obtained using boundary mismatch approximation is 43% larger than the actual value, which was acquired from the wire-heater method. Empirically, we obtain $\alpha = 1.6$ for the new *corrected* boundary mismatch approximation [Eq. (10)]. In other words, the approximation used by Moon it *et al.*[5] gives a value that is 60% larger than the actual $\kappa_l$.

Since we have the exact solution for the 2-medium problem [Eq. (11)], we can indeed fit $V_{s+l}$ using the value $\kappa_l = 0.063$ W m$^{-1}$ K$^{-1}$ and the value $\mathcal{R} = 5.0 \times 10^{-7}$ m$^2$ K/W which was obtained by fitting $V_s$ with Eq. (4). This fitting

gives $\kappa_s = 1.25\ \mathrm{W\,m^{-1}\,K^{-1}}$, in perfect agreement with the measured result without the liquid medium. Simulations show that $\alpha$ in Eq. (10) is a slowing varying coefficient vs the above parameters and is in good agreement with the experimentally determined value 1.6.[14] Further, the simulations demonstrate that the sensitivity of $\alpha$ on the above parameters decreases as the value of $b$ decreases, with $\mathcal{R}$ being the exception. The effect of interfacial thermal resistance scales as $\mathcal{R}/b$. For the parameters above, the optimal value of $b$ is approximately $b = 10\ \mu$m. In this case, $\alpha$ varies slowly from 1 to 1.1 when $\kappa_l/\kappa_s$ decreases from 1 to 0.05. The heater half-width $b$ used by Moon *et al.* is 30 $\mu$m[5] and the deviation of $\alpha$ from 1 is acceptable.

## ACKNOWLEDGMENTS

F.C. would like to thank Professor Kevin L. Stokes and Dr. Chuan Hu for the introduction to the $3\omega$ technique. The work is supported by NSF Grant No. DMR-9804325, the T. L. L. Temple Foundation, the John J. and Rebecca Moores Endowment, the State of Texas through the Texas Center for Superconductivity at the University of Houston; and at Lawrence Berkeley Laboratory by the U.S. Department of Energy under Contract No. DE-AC03-76SF00098.

[1] S. Andersson and G. Bäckström, Rev. Sci. Instrum. **57**, 1633 (1986).
[2] O. Nilsson, O. Sandberg, and G. Bäckström, Rev. Sci. Instrum. **57**, 2303 (1986).
[3] D. G. Cahill and R. O. Pohl, Phys. Rev. B **35**, 4067 (1987).
[4] D. G. Cahill, Rev. Sci. Instrum. **61**, 802 (1990).
[5] I. K. Moon, Y. H. Jeong, and S. I. Kwun, Rev. Sci. Instrum. **67**, 29 (1996).
[6] C. W. Chu and L. R. Testardi, Phys. Rev. Lett. **32**, 766 (1974).
[7] F. Chen, Q. M. Lin, Y. Y. Xue, and C. W. Chu, Physica C **282**, 1245 (1997).
[8] I. R. Walker, Rev. Sci. Instrum. **70**, 3402 (1999).
[9] H. S. Carslaw and J. C. Jaeger, *Conduction of Heat in Solids* (Oxford University Press, Oxford, 2001).
[10] J. H. Kim, A. Feldman, and D. Novotnyn, J. Appl. Phys. **86**, 3959 (1999).
[11] N. O. Birge, Phys. Rev. B **34**, 1631 (1986).
[12] In Ref. 9 Eq. (7.3.16).
[13] Bernd Lorenz (private communication).
[14] The values that we used are: $\kappa_s = 1.25\ \mathrm{W\,m^{-1}\,K^{-1}}$, $(\rho C)_s = (\rho C)_l = 2.0\ \mathrm{J/cm^3}$, $b = 45\ \mu$m, and $\mathcal{R} = 5.0 \times 10^{-7}\ \mathrm{m^2\,K/W}$.